THE JOURNAL OF BIOLOGICAL CHEMISTRY VOL. 282, NO. 44, pp. 32480–32490, November 2, 2007

A Caspase-3-cleaved Fragment of the Glial Glutamate Transporter EAAT2 Is Sumoylated and Targeted to Promyelocytic Leukemia Nuclear Bodies in Mutant SOD1-linked Amyotrophic Lateral Sclerosis*

Received for publication, May 25, 2007, and in revised form, September 4, 2007 Published, JBC Papers in Press, September 6, 2007, DOI 10.1074/jbc.M704314200

Stuart L. Gibb[‡§], William Boston-Howes[§], Zeno S. Lavina[¶], Stefano Gustincich[¶1], Robert H. Brown, Jr.[§2], Piera Pasinelli[‡], and Davide Trotti[‡3]

From the [‡]Farber Institute for Neurosciences, Weinberg Unit for ALS Research, Thomas Jefferson University, Philadelphia, Pennsylvania 19107, the [§]Cecil B. Day Laboratory for Neuromuscular Research, Massachusetts General Hospital and Harvard Medical School, Charlestown, Massachusetts 02129, and [¶]Scuola Internazionale Studi Superiori Avanzati, Sector of Neurobiology, The Giovanni Armenise-Harvard Foundation Laboratory, AREA Science Park, 34012 Basovizza, Italy

EAAT2 (excitatory amino acid transporter 2) is a high affinity, Na^+-dependent glutamate transporter of glial origin that is essential for the clearance of synaptically released glutamate and prevention of excitotoxicity. During the course of human amyotrophic lateral sclerosis (ALS) and in a transgenic mutant SOD1 mouse model of the disease, expression and activity of EAAT2 is remarkably reduced. We previously showed that some of the mutant SOD1 proteins exposed to oxidative stress inhibit EAAT2 by triggering caspase-3 cleavage of EAAT2 at a single defined locus. This gives rise to two fragments that we termed truncated EAAT2 and COOH terminus of EAAT2 (CTE). In this study, we report that analysis of spinal cord homogenates prepared from mutant G93A-SOD1 mice reveals CTE to be of a higher molecular weight than expected because it is conjugated with SUMO-1. The sumoylated CTE fragment (CTE-SUMO-1) accumulates in the spinal cord of these mice as early as presymptomatic stage (70 days of age) and not in other central nervous system areas unaffected by the disease. The presence and accumulation of CTE-SUMO-1 is specific to ALS mice, since it does not occur in the R6/2 mouse model for Huntington disease. Furthermore, using an astroglial cell line, primary culture of astrocytes, and tissue samples from G93A-SOD1 mice, we show that CTE-SUMO-1 is targeted to promyelocytic leukemia nuclear bodies. Since one of the proposed functions of promyelocytic leukemia nuclear bodies is regulation of gene transcription, we suggest a possible novel mechanism by which the glial glutamate transporter EAAT2 could contribute to the pathology of ALS.

Amyotrophic lateral sclerosis (ALS)[4] is a fatal neurodegenerative disease, resulting from a progressive death of cortical and spinal motor neurons. About 90% of ALS cases are sporadic, whereas the remaining 10% are inherited in a dominant manner (familial ALS). Transgenic expression of high levels of human mutant SOD1 (mutSOD1) proteins in mice and rats leads to a progressive motor neuron disease that shares most of the clinical features of ALS (1, 2). Astrocytes are essential partners of motorneurons, providing them with trophic support (3) and mediating rapid clearance of synaptic glutamate mainly through the action of glial glutamate transporters. The EAAT2 (excitatory amino acid transporter 2) glial isoform of glutamate transporters accounts for ~95% of total glutamate uptake activity in the brain (4). Studies in mutSOD1 mice and in *in vitro* models of ALS affirmed a role for astroglial involvement in motorneuron death and suggested that motorneuron loss is also the result of toxic contributions of nonneuronal cells of the spinal cord (5–8). Reactive astrocytes surrounding motorneurons contain protein inclusions; express inflammatory markers, such as the inducible forms of nitric oxide synthase and cycloxygenase-2; and display increased neural growth factor synthesis (9), nitrotyrosine immunoreactivity, and down-regulation of EAAT2. Excitotoxicity caused by consistent reduction in expression levels and activity of EAAT2 is among various proposed mechanisms implicated in the propagation of motorneuron death in ALS (10, 11). Studies of mutSOD1 models of ALS and human post-mortem specimens consistently reported impairment in EAAT2 expression levels (2, 12, 13). Two studies in mutSOD1 mice in which the expression levels of EAAT2 were genetically modified concluded that EAAT2 plays a role in modifying the motor neuron loss and the progression of the disease (14, 15).

* This work was supported in part by National Institutes of Health Grant RO1-NS44292 (to D. T.), the Muscular Dystrophy Association (to D. T.), and the ALS Association (to D. T. and P. P.). The Weinberg Unit for ALS Research was also supported by the Farber Family Foundation. The costs of publication of this article were defrayed in part by the payment of page charges. This article must therefore be hereby marked "*advertisement*" in accordance with 18 U.S.C. Section 1734 solely to indicate this fact.

[1] Supported by Telethon Italia Grant GGP06268, GRAND, and the "Giovanni Armenise-Harvard Foundation."

[2] Supported by NINDS, National Institutes of Health, the ALS Association, Project ALS, the de Bourgknecht ALS Research Fund, the Angel Fund, the Al-Athel ALS Research Foundation, and the ALS Therapy Alliance.

[3] To whom correspondence should be addressed: Farber Institute for the Neurosciences, Weinberg Unit for ALS Research, Thomas Jefferson University, 900 Walnut St., Philadelphia, PA 19107. Tel.: 215-955-8416; Fax: 215-503-9128; E-mail: davide.trotti@jefferson.edu.

[4] The abbreviations used are: ALS, amyotrophic lateral sclerosis; SOD1, Cu^{2+}/Zn^{2+} superoxide dismutase; mutSOD1, mutated SOD1; WT-SOD1, wild type SOD1; SUMO, small ubiquitin modifier protein; PML, promyelocytic leukemia; PML-NB, PML nuclear body; E1, ubiquitin-activating enzyme; E2, ubiquitin carrier protein; E3, ubiquitin-protein isopeptide ligase; PBS, phosphate-buffered saline; CTE, COOH terminus of EAAT2; CHAPS, 3-[(3-cholamidopropyl)dimethylammonio]-1-propanesulfonic acid; mAb, monoclonal antibody; HD, Huntington disease; EGFP, enhanced green fluorescent protein; Tricine, *N*-[2-hydroxy-1,1-bis(hydroxymethyl)ethyl]glycine; DAPI, 4′,6-diamidino-2-phenylindole.

We have recently demonstrated that caspase-3 cleaves EAAT2 at a unique site located in the cytosolic COOH terminus of the transporter, a finding that could link excitotoxicity and activation of caspase-3 as converging mechanisms in the pathogenesis of ALS. In addition, we have found that mutSOD1 proteins inhibit EAAT2 via a mechanism that largely involves activation of caspase-3 and cleavage of the transporter (16). In this report, we demonstrate that the caspase-cleaved fragment of EAAT2 (CTE) is modified by small ubiquitin-related modifier (SUMO)-1. Covalent attachment of SUMO (sumoylation) to proteins or peptides is a reversible post-translational modification. Sumoylation is analogous to ubiquitination, particularly since both mechanisms target lysine residues. The process of sumoylation requires an E1 activating enzyme (SAE1/SAE2), an E2 conjugating enzyme (Ubc9) and possibly a member from the family of E3 ligases (17). Attachment of SUMO requires a lysine residue that is located within a SUMO consensus motif, ψKXE. The motif is somewhat flexible, since ψ represents a large hydrophobic residue and X can be any residue (18, 19). Deconjugation is carried out by SUMO-specific proteases (20). As with ubiquitin, there are many substrates for SUMO; many functions for sumoylation have been assigned, including antagonism to ubiquitin (21), alteration of subcellular localization of target substrates (22), regulation of transcriptional factor activity (23), functional alterations of plasma membrane channels (24, 25), and modulation of nuclear pore complex shuttling (26).

We present evidence that the sumoylated CTE species is targeted to a subnuclear structure known as promyelocytic leukemia (PML) nuclear bodies. PML nuclear bodies (PML-NBs) are subnuclear structures made of PML protein held together by SUMO-1 (27). Many sumoylated proteins are targeted to these structures (17). The exact array of functions assigned to PML-NBs, however, remains to be fully elucidated. Taken together, our observations that a proteolytic fragment of EAAT2 is sumoylated, accumulates during the course of ALS, and localizes to PML-NBs argue that it may play an active role in the pathogenesis of the disease. In support of this, there is a growing body of evidence reporting protein sumoylation as a post-translational mechanism implicated in a number of neurodegenerative disorders, including ALS (28).

EXPERIMENTAL PROCEDURES

Animals—Wild type human SOD1 and G93A-SOD1 transgenic mice, nontransgenic (non-TgN) control mice, H46R-SOD1 transgenic rats, and the R6/2 mouse model of Huntington disease were used for this study. The mouse colonies B6SJL-TgN(G93A-SOD1)1Gur and B6SJL-TgN(SOD1)2Gur (stock numbers 002726 and 002297; Jackson Laboratories) were expanded and maintained in house. The rat line was H46R-4 carrying 25 copies of the transgene (29). R6/2 mice were obtained from Dr. Jonathan Fox (MGH).

Astrocyte Preparation—Cortices or spinal cords were removed from postnatal day 1–2 non-TgN mice and placed in ice-cold Hanks' solution (Invitrogen). After washing in PBS/glucose solution, the tissue was digested for 3 min in Dulbecco's modified Eagle's medium/trypsin/DNase solution, washed in PBS/glucose, and then triturated by passing the tissue several times through a 20-gauge needle in Dulbecco's modified Eagle's medium/DNase solution (Dulbecco's modified Eagle's medium was from Invitrogen; trypsin and DNase were from Worthington). The homogenate was then filtered through a 100-μm cell strainer, centrifuged, and resuspended in Dulbecco's modified Eagle's medium, 10% fetal bovine serum, 2% glucose. Astrocytes were grown on poly-D-lysine cultureware (Millipore) and were typically maintained in culture for 1–2 weeks prior to use for transfections. Cultures were passed once before transfection.

Constructs, Transfections, and Protein Extraction—Full-length EAAT2, CTE (amino acids 506–574 of EAAT2), His-CTE-SUMO-1 fusion fragment, Ubc-9, and His-SUMO-1 cloned into pcDNA3.1 were transiently transfected in HEK 293 cells, U251 cells, or primary astrocytes as indicated using Lipofectamine 2000 (Invitrogen). CTE and CTE-SUMO-1 coding regions were generated by PCR, and the cDNAs were subcloned in pcDNA3.1. A Kozak initiation sequence and an artificial start codon were placed at the 5′-end of the CTE and CTE-SUMO-1 sequence. Transfected cells were harvested after 48 h in CHAPS extraction buffer, briefly sonicated, and analyzed on Western blot or stored at −80 °C. Separation of cytoplasmic and nuclear fractions from cultured cells and tissues was achieved with the NE-PER kit (Pierce) according to the manufacturer's instructions.

Antibodies—The following antibodies were used for Western blot applications. A polyclonal antibody raised against the last 17 amino acids of rat EAAT2 COOH terminus was purchased from Affinity BioReagent (catalog number PA3-040), which we termed ABR556–573 (1:1,000–10,000). The polyclonal B 493–508 (rabbit 84946) and B 12–26 (rabbit 26970) antibodies against rat EAAT2 were generous gifts from Dr. N. C. Danbolt and characterized in his laboratory (30–32). The antibody ABR518-536 was produced by Affinity BioReagent (15 mg/ml). This is a polyclonal, affinity-purified anti-peptide antibody raised in rabbits against the mouse EAAT2 amino acid sequence TQSIYDDKNHRESNSNQC located downstream from the caspase-3 consensus site at positions 518–536 of the mouse EAAT2 transporter (see Fig. 1*A*). The optimal working concentration was determined to be 0.1 μg/ml. All of the anti-EAAT2 antibodies that are available for this study react with human, mouse, and rat EAAT2 isoforms. Other antibodies used in this study include anti-GM130 mAb (monoclonal; BD Biosciences; 1:250), anti-histidine tag mAb (monoclonal; Sigma; 1:50,000), anti-PML mAb (monoclonal; Millipore; 1:200–500), anti-SUMO-1 mAb (monoclonal; Invitrogen; clone 21C7, 1:200), anti-poly(ADP-ribose) polymerase mAb (monoclonal; BD Biosciences; 1:500), and anti-monoubiquitin and anti-polyubiquitin mAbs (monoclonal; Affinity Research Products; clone FK2; 1:500).

Immunofluorescence—Astrocytes grown on poly-D-lysine-coated coverslips were fixed 48 h after transfection. Cells were washed twice with PBS and then fixed with freshly prepared 4% paraformaldehyde for 10 min at room temperature. Cells were permeabilized and blocked overnight with 0.5% Triton X-100 and 10% goat serum in PBS. Cells were incubated with anti-PML antibody in PBS with 0.1% Triton X-100 and 1% goat serum for 1 h at room temperature before washes in PBS. Secondary antibody (anti-mouse AlexaFluor568; Invitrogen) was

also incubated for 1 h in PBS with 0.1% Triton X-100 and 1% goat serum before PBS washes. Cells were then mounted in Vectorshield containing 4′,6-diamidino-2-phenylindole (DAPI) (Vector Laboratories) on Superfrost Plus coverslips (Fisher). EGFP-CTE-SUMO-1 expression was detected by fluorescence.

Immunoprecipitations—Aliquots of spinal cord homogenates (CHAPS extracts) were diluted in radioimmune precipitation buffer and cleared overnight at 4 °C with protein A or G magnetic beads (New England Biolabs, Ipswich, MA). Homogenates were then incubated for 4 h at 4 °C with the appropriate antibody or control immunoglobulins, and the immunocomplexes were precipitated by the addition of 25 μl of protein A or G magnetic beads for 1 h at 4 °C. The beads were then washed three times with 0.5 ml of ice-cold radioimmune precipitation buffer and boiled for 5 min in SDS-sample buffer. Supernatants were analyzed on Western blot and developed with ECL (Amersham Biosciences).

Selective Yeast Two-hybrid Screen—EAAT2 sequence was amplified from pcDNA3.1-EAAT2 using Platinum *Pfx* DNA polymerase (Invitrogen) and the following primers: EAAT2-Forward (AAGAATTCTCAGTCAATGTTGTGGGTGAC) and EAAT2-Reverse (AAGCGGCCGCTTATTTCTCACGTTTCCAAG). The two primers contain a restriction site for EcoRI and NotI, respectively, and allow the amplification of the cytoplasmic COOH-terminal region of EAAT2 from amino acid 480 to 574. 25 cycles were performed (94 °C for 15 s, 55 °C for 30 s, 68 °C for 1 min). The amplification product was subcloned into pGEM-T Easy Vector (Promega) and then inserted into the yeast vector pEG202 by EcoRI/NotI digestion in frame with the sequence coding for LexA. The cell lysate was used to perform Western blot analysis using an anti-LexA antibody to test bait expression. A protein of the expected size was detected only in the bait strain. Autoactivation tests were performed to ensure that the bait in pEG202 did not activate the *lacZ* reporter by itself or that EGY48, which contains *LEU2*, is an appropriate strain for the bait. We used the bait strain EGY48 MATα containing the *lacZ* reporter plasmid (pSH18–34) and the bait-expressing plasmid (pLexA-EAAT2 480–574). The EGY48/pSH18–34/pLexA-EAAT2 480–574 yeast strain was transformed with several constructs isolated from a human fetal brain cDNA library cloned into pJG4-5. The interactions were assayed as previously described (33). B42-fused proteins were expressed from the yeast GAL1 promoter: on in galactose but off in glucose. All transformations were screened for *lacZ* and *Leu2* expression, which indicated the association of B42-fused proteins with LexA-EAAT2. *lacZ* and *Leu2* expression was evaluated by blue-staining on 5-bromo-4-chloro-3-indolyl-β-D-galactopyranoside (X-gal)-containing plates and growth on medium lacking leucine.

In Vitro Cleavage Reactions—Mice were euthanized by intraperitoneal injection of xylazine/ketamine. Spinal cords were collected and immediately homogenized on ice (glass-Teflon homogenizer; 1,000 rpm) in 30 volumes of extraction buffer containing SDS or CHAPS (1%), 150 mM NaCl, 10 mM NaP_i (pH 7.4), and Complete™ protease inhibitor mix with EDTA (Roche Applied Science). "Crude" extracts were incubated for 10 min at room temperature, briefly sonicated, centrifuged (1,000 × *g*, 4 min) to remove unsolubilized material, and immediately analyzed or stored at −80 °C. The homogenates prepared with the above protocol were termed SDS or CHAPS extracts. For the caspase cleavage experiments, 5 μl of CHAPS extract, containing 10–25 μg of total proteins, were incubated for 2 h at 37 °C in 50 μl of caspase cleavage buffer containing 10% sucrose, 20 mM HEPES/Na (pH 7.4), 100 mM NaCl, 1 mM EDTA, 10 mM DTT, the protease inhibitor mixture (Complete™ with EDTA) in the presence or absence of purified human recombinant active caspases (BD Biosciences). The Complete™ inhibitor mixture did not inhibit caspase-3 (16). Calpain I and II cleavage reactions were run at room temperature for 1 h in 50 μl of buffer containing 100 mM imidazole (pH 7.4), 5 mM cysteine, and 5 mM $CaCl_2$. Reactions were terminated by adding SDS-containing sample buffer and boiling for 5 min and then analyzed by Western blot.

In Vitro Sumoylation of EAAT2 and CTE Fragment—HEK 293 cells were grown to ~80% confluence and transfected with pcDNA 3.1-EAAT2 or pcDNA 3.1-CTE in the presence or absence of pcDNA3-His-SUMO-1 and pcDNA3-Ubc9, 1 μg of DNA for each construct. In the EAAT2 group, 2 μg of DNA of empty vector were added to balance out the total amount of DNA added to the different groups. Cells were lysed in PBS buffer containing 1% Triton X-100, protease inhibitors (Complete™ EDTA-free), 20 mM NEM (to inhibit SUMO proteases) and homogenized, followed by sonication. An aliquot of homogenate was directly loaded on a 10% gel to determine the level of expression of EAAT2 or CTE fragment. One mg of protein from the homogenate was then loaded on a nickel spin column (catalog number H7787; Sigma), and the His-tagged proteins retained by the column were eluted with 500 μl of 250 mM imidazole buffer following the manufacturer's instructions. 30–40 μl of the eluate was then analyzed by Western blot with different antibodies as indicated.

RESULTS

A Fragment Derived from Caspase-3 Cleavage of the Cytoplasmic COOH-terminal Domain of EAAT2 Accumulates in the Spinal Cord of ALS Mice at a Molecular Weight Larger than Expected—Using site-directed mutagenesis, we have previously shown that caspase-3 cleaves the glutamate transporter EAAT2 at a unique consensus site located in its cytoplasmic COOH-terminal domain (16). Caspase-3 cleavage of *in vitro* translated EAAT2 generated two fragments, (Tr)EAAT2 and CTE, with molecular masses of ~55 and 8 kDa, respectively (16) (Fig. 1*A*).

We looked for the presence of the (Tr)EAAT2 form in spinal cord homogenates of G93A-SOD1 mice at different stages of disease and previously reported a progressive loss of EAAT2 immunoreactivity with the antibody B 12–26, which also detected a slight accumulation at progression of disease of a 55 kDa band corresponding to the (Tr)EAAT2 fragment (16). Interestingly, when the same sample homogenates were probed with the ABR 556–573 antibody (the epitope of which is directed against the last 16 amino acids of the EAAT2 COOH terminus; see Fig. 1*A*) looking for the CTE fragment, we observed a broad band centered at ~25 kDa, accumulating presymptomatically and increasing in intensity as the disease progressed (Fig. 1, *B* and *C*). This band was also detected by another antibody, the ABR 518–536, whose epitope is within

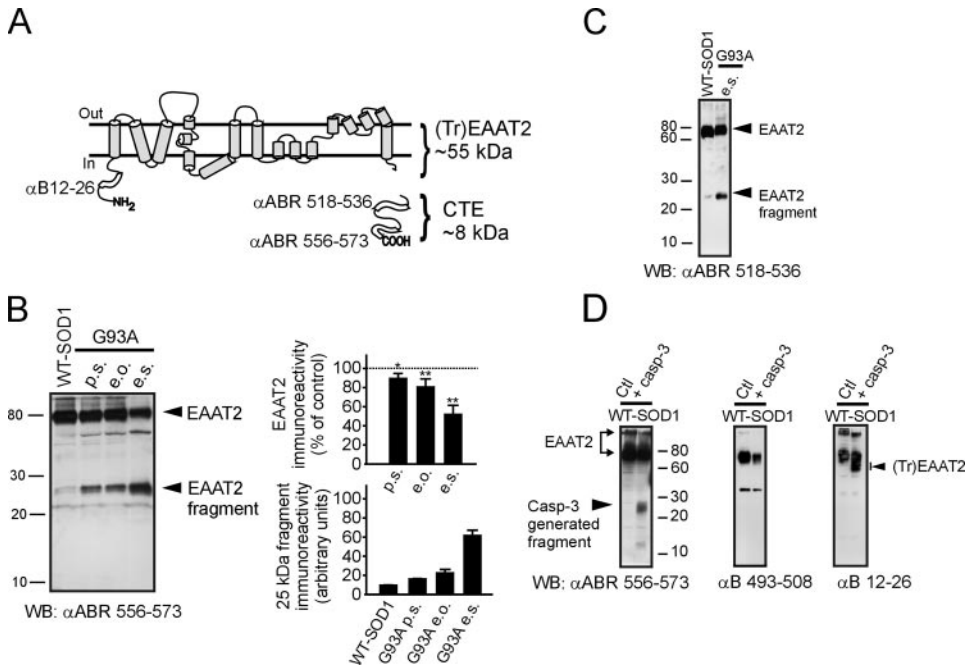

FIGURE 1. **Caspase-3 cleaves EAAT2 at the caspase-3 consensus motif located in the cytoplasmic COOH-terminal domain of the transporter.** *A*, topological organization of EAAT2 at the plasma membrane as deduced from crystallographic data; the figure illustrates the theoretical size of fragments generated by caspase-3 cleavage and the epitopes of the anti-EAAT2 polyclonal antibodies used in this study (34). *B*, Western blot (*WB*) analysis (16.5% Tris-Tricine gel) of spinal cord homogenates from G93A-SOD1 at different stages of disease progression (*p.s.*, presymptomatic stage, 70 days old; *e.o.*, early symptomatic, 100 days old; *e.s.*, end stage, ~130 days old) and human WT-SOD1 mouse spinal cord homogenate age-matched with end stage G93A-SOD1 mice. Homogenates were probed with the carboxyl-terminal antibody ABR 556–573 (1:1,000); human WT-SOD1 homogenates were used as a control. *C*, Western blot analysis (SDS-PAGE, 12% gel) of spinal cord homogenates prepared from G93A-SOD1 end stage and age-matched WT-SOD1 mice probed with the carboxyl-terminal antibody ABR 518–536 (0.1 μg/ml). *D*, Western blot analysis (12% Tris-glycine gel) of WT-SOD1 spinal cord homogenates treated with active recombinant caspase-3 (200 ng, 37 °C, 2 h) and probed with the antibodies B 493–508 (0.1 μg/ml) and B 12–26 (0.2 μg/ml). B 493–508 also identifies a band just above 30 kDa. This band is unlikely to be related to the EAAT2 transporter (32), and it does not accumulate in the G93A-SOD1 mice at disease progression (see Fig. 7, *D* and *E*, in Ref. 16).

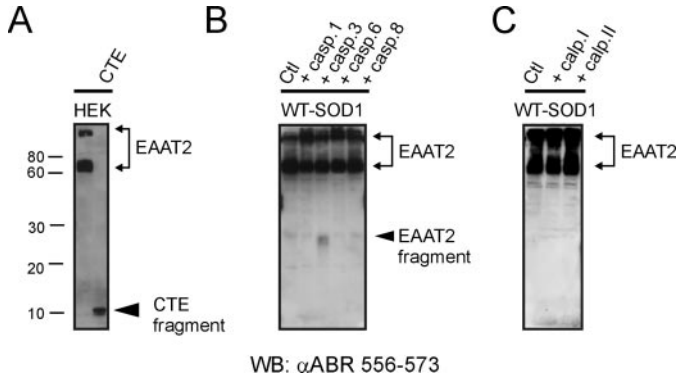

FIGURE 2. **25-kDa CTE is not due to aggregation and is generated by caspase-3-mediated cleavage.** *A*, HEK 293 cells were transiently transfected with EAAT2 and CTE cDNAs in pcDNA3.1 plasmid (1 μg/well). Despite conditions that favor aggregation of EAAT2, CTE runs as a monomer at the expected apparent molecular mass. *B*, Western blot (*WB*) analysis of spinal cord homogenates from WT-SOD1 overexpressor mice treated with active recombinant caspases (200 ng, 37 °C, 2 h). Only caspase-3 generates the 25-kDa fragment. *C*, Western blot analysis of spinal cord homogenates from WT-SOD1 overexpressor mice treated with active recombinant calpain I and calpain II (Calbiochem) (200 ng, room temperature, 1 h). No fragments of EAAT2 were generated with either calpains. *Ctl*, control.

the CTE fragment but downstream of the caspase-3 cleavage site (Fig. 1*C*). ABR 518–536 also detected a similar 25 kDa band in spinal cord homogenates of symptomatic H46R-SOD1 rats (data not shown). Accumulation of the 25 kDa band was paralleled by a concomitant decrease in full-length EAAT2 monomer (Fig. 1*B*), suggesting that the appearance of the lower band and the disappearance of EAAT2 monomer were related events occurring during disease progression.

We initially investigated the nature of the 25-kDa fragment using mass spectrometry. However, this approach was not successful because of the insufficient yield of fragment immunopurification. As an alternative, we tried an approach based on correlative evidence. We treated spinal cord homogenates of WT-SOD1 mice with active recombinant caspase-3. The treatment generated a broad band centered at 25 kDa, which was immunostained by ABR 556–573 and not by B 493–508 (the epitope of which spans the caspase-3 cleavage consensus site) or the NH_2 terminus B 12–16 antibody (Fig. 1*D*). In addition to the uncleaved EAAT2, the antibody B 12–26 also immunostained (Tr)EAAT2 (Fig. 1*D*, *right*, *arrow*), suggesting that caspase-3 was cleaving at its canonical motif in the EAAT2 COOH terminus, whereas the B 493–508 antibody, despite detecting a decrease in EAAT2 monomer, did not recognize the fragment at 25 kDa as one would expect if caspase-3 were to cleave at the consensus site within the B 493–508 epitope (Fig. 1*D*, *middle*). The size of the fragment generated *in vitro* in spinal cord (25 kDa) matched the size seen *in vivo*, strongly suggesting that the EAAT2 fragment in the spinal cord of ALS mice was derived from caspase-3 cleavage. Caspase-3 cleaved *in vitro* translated [^{35}S]EAAT2 at the predicted consensus site and generated a fragment of ~10 kDa (16). To account for the size discrepancy, one must consider the possibility that in a biological system, this fragment forms an irresolvable, SDS-resistant aggregate, or EAAT2 is cleaved at a different locus by other proteases or caspases that are activated by the active caspase-3 added to the cleavage reaction, or the EAAT2 fragment is post-translationally modified.

EAAT2 has a tendency to aggregate on gel-forming dimers and trimers, reflecting its native oligomeric assembly (34). To determine whether the band at 25 kDa represented oligomeric aggregation of the CTE fragment, we transfected HEK 293 cells with the construct encoding for the CTE fragment and analyzed the CHAPS extract on Western blot with the ABR 556–573 antibody. The analysis showed that CTE runs as a single band at ~10 kDa, although the conditions of the experiment allowed aggregation of the full-length EAAT2 (Fig. 2*A*), negating the

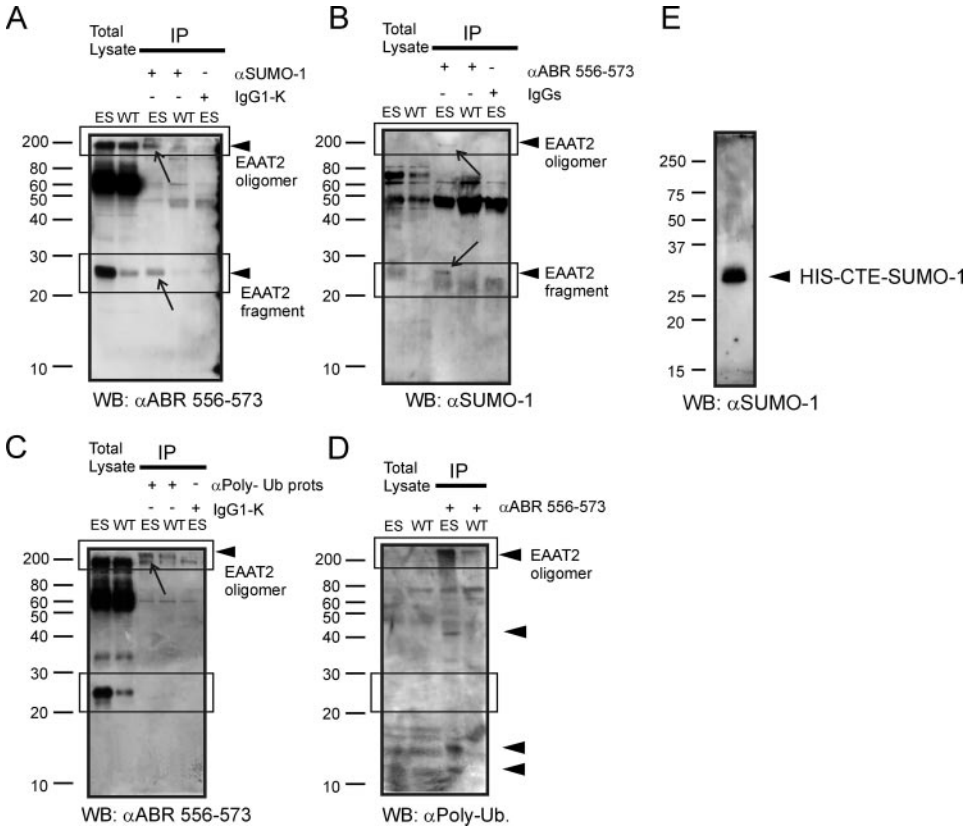

FIGURE 3. **The 25-kDa EAAT2 fragment is post-translationally modified by SUMO-1 conjugation.** *A*, spinal cord homogenates of end stage G93A-SOD1 (*ES*) and age-matched WT-SOD1 (*WT*) mice (500 μg of total proteins) were immunoprecipitated (*IP*) with 5 μg of monoclonal antibody anti-SUMO-1. The immunoprecipitate was then separated on a 12% gel and probed (*WB*) with ABR 556–573. As control, we performed the immunoprecipitation from a spinal cord homogenate of G93A-SOD1 end stage with 5 μg of purified mouse IgG1-k (catalog number 01-6100; Zymed Laboratories Inc.), the same isotype as of the anti-SUMO-1 antibody. In addition to the 25-kDa fragment (*bottom*), a portion of EAAT2, visible as a high molecular weight aggregate, was sumoylated at end stage (*top*). *B*, 10 μl of ABR 556–573 were used to immunoprecipitate spinal cord homogenates from the same samples as in *A*. The immunoprecipitates were separated on 12% gel and probed with anti-SUMO-1 antibody. *C* and *D*, forward and reverse immunoprecipitation of spinal cord homogenates with a monoclonal antibody raised against poly- and monoubiquitinated proteins (5 μg, isotype IgG1-k) and the ABR 556–573 antibody (10 μl). In the G93A-SOD1 end stage, a fraction of EAAT2 was polyubiquitinated if compared with WT-SOD1 age-matched control. This is shown by the immunopositivity of high molecular weight aggregates. In addition, several EAAT2 fragments were also ubiquitinated at end stage, suggesting an active degradation of the transporter via the ubiquitin pathway. Despite this, the 25-kDa fragment was not immunoprecipitated by the polyubiquitin antibody. *E*, HEK 293 cells were transiently transfected with His-CTE-SUMO-1 fusion construct in pcDNA 3.1 (1 μg/well). The CHAPS extract homogenate was analyzed on Western blot with the anti-SUMO-1 antibody.

possibility that the 25 kDa band seen *in vivo* represented an oligomeric aggregate of CTE. It also seems unlikely that the 25-kDa fragment derived from other protease activity, since the caspase-3 cleavage was performed in the presence of a wide range of protease inhibitors, including inhibitors of metal-dependent proteases. Caspase-3 could promote indirect cleavage of EAAT2 at an upstream cleavage site by activating other caspases or calpains (35). Again, this should not be the case, since EAAT2 is not sensitive to cleavage by other caspases, such as caspase-1, -6, -8 (Fig. 2*B*) or -7 (16) as well as calpain I and II (Fig. 2*C*). It therefore seems unlikely that the 25-kDa fragment derived either from the proteolytic activity of these caspases or calpains.

Sumoylation of the Caspase-3-derived EAAT2 Proteolytic Fragment—Considering the data presented in Figs. 1 and 2, the most compelling explanation for the size difference is that CTE is modified by post-translational conjugation. On this premise, we set out to determine whether the CTE fragment was covalently attached to ubiquitin and/or ubiquitin-like SUMO proteins. These two post-translational modifications occur at lysine residues. The CTE fragment has 6 lysine residues, including a canonical consensus site for sumoylation (ψK*X*E) (20), represented by the sequence WKREK located at the very end of the EAAT2 COOH terminus domain. To test whether the CTE fragment was ubiquitin- or SUMO-conjugated, spinal cord homogenates from end stage G93A-SOD1 and age-matched WT-SOD1 mice were immunoprecipitated with monoclonal antibodies against SUMO-1 and ubiquitin (anti-ubiquitin and poly- and monoubiquitinated proteins). The anti-SUMO-1 antibody predominantly immunoprecipitated a band centered at 25 kDa in the G93A-SOD1 end stage sample that was detected by the ABR 556–573 polyclonal antibody (Fig. 3*A*), suggesting that this fragment was indeed SUMO-1-conjugated. Reverse immunoprecipitation with the antibody ABR 556–573 pulled down a band immunostained by SUMO-1 antibody with an apparent molecular mass of 25 kDa (Fig. 3*B*). Furthermore, bands were also observed at high molecular masses (>200 kDa), perhaps indicating sumoylation of the EAAT2 homotrimer. In contrast, immunoprecipitation reactions in either direction failed to produce detectable bands in WT-SOD1 mice, suggesting a distinct difference between WT-SOD1 and G93A-SOD1 end stage samples. The antibody raised against ubiquitinated proteins also failed to immunoprecipitate a detectable band at 25 kDa (Fig. 3*C*). A reverse immunoprecipitation experiment confirmed that the CTE fragment at 25 kDa was not ubiquitinated (Fig. 3*D*). Instead, several other bands at low (≤17 kDa) and high (≥43 kDa) molecular mass were immunoprecipitated, suggesting active proteolytic degradation and ubiquitination of EAAT2 at disease end stage (Fig. 3*D*). These ubiquitinated EAAT2 fragments were not present at presymptomatic and early stages (data not shown). We also tested whether CTE could be modified by SUMO-2 and SUMO-3 but found no evidence of such interaction (data not shown). Attachment of SUMO-1 to the CTE fragment would theoretically increase the molecular mass by ~11 kDa. However, because SUMO-1 runs aberrantly on gel at ~17 kDa (data not shown) (36), the resulting apparent molecular mass would

be ~25 kDa. To test this possibility, we generated an in-frame fusion of our species of interest with SUMO-1 (37). The approach of constructing a CTE-SUMO-1 in-frame fusion protein was deemed appropriate, since the sumoylation consensus site in EAAT2 is at the very end of the COOH-terminal domain. The chimeric construct of CTE and SUMO-1 was subsequently cloned in pcDNA3.1 His tag vector. Western blot analysis of CHAPS extract of HEK 293 cells transfected with CTE-SUMO-1 revealed an apparent molecular mass of 30 kDa, which corresponded to the 25-kDa fragment plus ~5 kDa due to the extra 40 amino acids introduced into the construct by the cloning procedure (Fig. 3*E*). Taken together, these observations suggest that CTE is sumoylated, giving rise to specie that run at ~25 kDa on Western blots.

EAAT2 COOH Terminus Interacts with Proteins of the SUMOylation Machinery—For sumoylation to occur, enzymes that promote the attachment of SUMO must be able to bind EAAT2. To assess whether this was the case, we screened a selective library of cDNA clones encoding proteins involved in the sumoylation pathway, along with several other proteins involved in neurodegenerative diseases, for their potential interaction with the COOH terminus of EAAT2. The COOH-terminal region of EAAT2 (amino acids 480–574) was fused to LexA and used as bait in a yeast two-hybrid screening experiment. The EGY48/pSH18–34/pLexA-EAAT2 480–574 yeast strain was transformed with pB42-SUMO-1 (accession number BC053528), ubiquitin-related protein, pB42-hUbc9 (accession number BT007010; SUMO-conjugating enzyme E2), and other preys. pLexA-EAAT2 480–574 strongly interacts with pB42-SUMO-1 and pB42-Ubc9, whereas no interaction was observed with preys like pB42-ferritin and pB42-ddx41 (Table 1). pB42-SUMO-1 and pB42-Ubc9 showed no interactions with pLexA-rrs1 (regulator of ribosome synthesis 1), pLexA-αsynA53T, and pLexA. The interaction between LexAp53 and pB42-LTSV40 was tested as a positive control for a strong interaction (38, 39). All interactions occurred only in the presence of galactose.

In Vitro SUMOylation of EAAT2 and the EAAT2-derived CTE Fragment—To further validate our data, we sought direct evidence for EAAT2 and CTE sumoylation *in vitro*. HEK 293 cells were co-transfected with cDNA encoding the CTE fragment or the EAAT2 transporter along with His-SUMO-1 and the E2-sumoylating enzyme, Ubc-9. His-sumoylated proteins were isolated from the cell homogenate by affinity purification with nickel columns. Western blot analysis of the eluate from CTE-expressing cells revealed a band migrating at 25 kDa immunostained by both the B 518–536 and the anti-SUMO-1 antibodies (Fig. 4*A*). We found that EAAT2 was also capable of being sumoylated *in vitro*, apparently even with higher efficiency than the CTE fragment. Similarly, transfection of HEK 293 cells with full-length EAAT2, Ubc-9, and His-SUMO-1 constructs led to sumoylation of EAAT2 (Fig. 4*B*). Overall, the lines of evidence collected thus far point at the conclusion that the glutamate transporter EAAT2 and its proteolytic derived fragment are sumoylated during the course of ALS and that this modification can be reconstituted in a model system.

TABLE 1

Yeast two-hybrid analysis of a selected library of cDNAs shows strong interaction of the EAAT2 COOH terminus with the SUMO-conjugating enzyme Ubc-9

A strong interaction with the COOH-terminal domain of EAAT2 was observed with Ubc-9, the SUMO-conjugating enzyme. The interaction was at least as strong as for LTSV40 for the oncogene p53, which was used as a positive control for our assay. SUMO-1 was also interacting, although less strongly, with the EAAT2 COOH-terminal domain. In the same assay, Ubc-9 did not interact with other baits like ferritin, Rrs1, or α-synuclein A53T. aa, amino acids.

Protein	Assay	Interaction
Bait: EAAT2 carboxyl-terminal domain (aa 480–574)		
Ubc9	β-Galactosidase	+++
	Leu	+++
SUMO1	β-Galactosidase	+++
	Leu	++
Ferritin	β-Galactosidase	–
	Leu	–
Ddx41	β-Galactosidase	–
	Leu	–
Rrs1	β-Galactosidase	–
	Leu	–
α-SynucleinA53T	β-Galactosidase	–
	Leu	–
LexA (−ve control)	β-Galactosidase	–
	Leu	–
Baits: Ferritin, Rrs1, α-synucleinA53T, Ddx41 (−ve controls)		
Ubc9	β-Galactosidase	–
	Leu	–
SUMO1	β-Galactosidase	
	Leu	–
Bait: p53 (+ve control)		
LTSV40	β-Galactosidase	+++
	Leu	+++

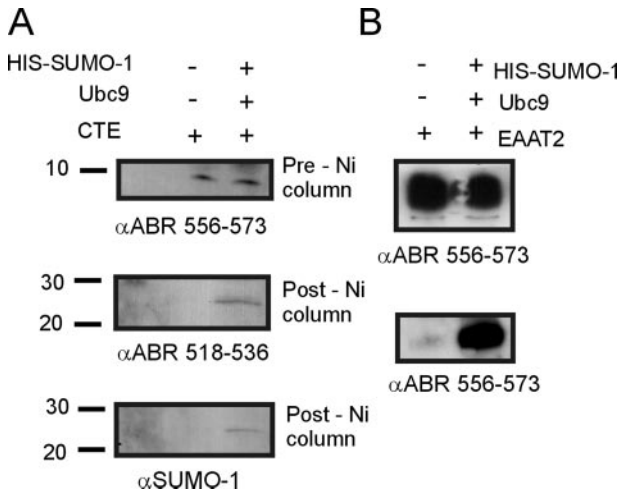

FIGURE 4. **The CTE carboxyl-terminal fragment of EAAT2 is sumoylated *in vitro*.** *A*, HEK 293 cells were co-transfected with CTE with or without His-SUMO-1 and Ubc-9 (*top*). Cell homogenates were affinity-purified through nickel (*Ni*) column chromatography to retain His-SUMO-1-tagged proteins. Postcolumn eluate was probed both with the anti-EAAT2 antibody B 518–536 (*middle*) and anti-SUMO-1 (*bottom*). *B*, the same experiment as in *A* except that HEK 293 cells were transfected with EAAT2. The postcolumn affinity-purified eluate was probed with the carboxyl-terminal antibody ABR 556–573.

Accumulation of the 25-kDa EAAT2 Fragment Occurs Selectively in Areas of the Central Nervous System Affected in ALS—The 25-kDa sumoylated fragment of EAAT2 accumulated in the spinal cord of G93A-SOD1 mice at higher levels compared with WT-SOD1 mice (Fig. 5*A*). No accumulation was noted in the hippocampus, cerebral cortex, or striatum (Fig. 5*B*). Interestingly, fragment accumulation was unique to ALS, since we

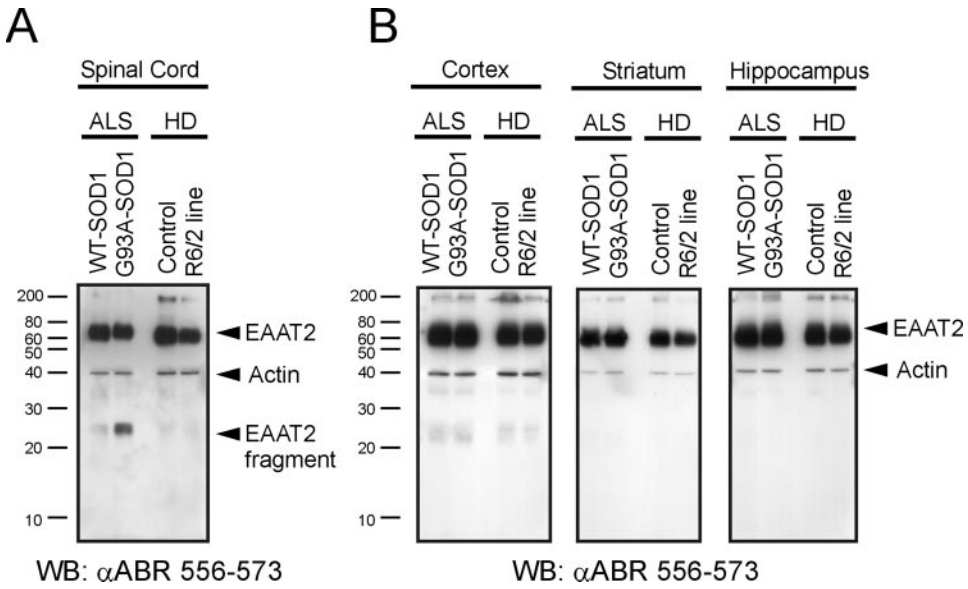

FIGURE 5. **Selective accumulation of the CTE fragment derived from caspase-3 cleavage in the spinal cord of ALS mice.** *A*, Western blot (*WB*) analysis of spinal cord homogenates (SDS extract) obtained from ALS mice (end stage G93A-SOD1 mice and age-matched control WT-SOD1) and Huntington disease mice (HD R6/2 line and nontransgenic control). The blot was co-stained with ABR 556–573 and β-actin antibodies. The β-actin signal was used as a marker of equal protein loading on the *lanes*. *B*, Western blots from cortex, striatum, and hippocampal homogenates (SDS extracts) were similarly probed as in *A*. The proteolytic EAAT2-derived fragment at 25 kDa is notably absent. Also absent is the increase in apparent molecular mass of the monomeric form of EAAT2 in the HD samples as compared with the spinal cord of ALS samples.

failed to detect the EAAT2 fragment in homogenates of CNS areas of the R6/2 mouse model of Huntington disease (HD) (Fig. 5, *A* and *B*). Moreover, we detected an upward shift of the band corresponding to EAAT2 monomer (Fig. 5*A*; see also Fig. 1*B*). This increase in apparent molecular weight of EAAT2 monomer was ALS- and spinal cord-specific. Despite the observation that HD and ALS mice shared a similar decrease in EAAT2 expression levels (40) (Fig. 5, *A* and *B*), our findings indicate that EAAT2 proteolytic processing differs between these two distinct neurodegenerative diseases.

CTE-SUMO-1 but Not CTE Accumulates in the Nucleus at PML Nuclear Bodies—We next sought to understand the effect of sumoylation by examining the cellular localization of CTE-SUMO-1 in contrast to the loci of CTE alone, since sumoylation has been previously reported to alter cellular localization of proteins (22). To this end, we transfected U251 astroglioma cells with His-tagged CTE and CTE-SUMO-1 in-frame fusion. We choose U251 as opposed to primary astrocytes, since the transfection efficiency of primary cultures is suboptimal for Western blot analysis. Fractionation of the transfected cells into cytoplasmic and nuclear components revealed a contrasting pattern between the two species with CTE remaining solely in the cytoplasm, whereas CTE-SUMO-1 was present in both fractions. To ensure that fractionation had taken place, separate aliquots were probed for cytoplasmic and nuclear markers (Fig. 6*A*). Given this observation, we sought to determine if this was repeated in the G93A mice. Analysis of end stage spinal cord homogenates revealed the band corresponding to CTE-SUMO-1 in both the cytoplasmic and the nuclear fraction (Fig. 6*B*); thus, one effect of sumoylation of CTE is a change in its cellular localization. The relative amounts of cytoplasm to nuclear staining were lower in the animal model when compared with the cell model. This was probably due to the fact that SUMO proteases can hydrolyze the modification in the animal, whereas the CTE-SUMO-1 species transfected into U251 cells is by its nature nonhydrolyzable.

To further pursue our investigation into the cellular loci of CTE-SUMO-1, we generated an EGFP-CTE-SUMO-1 vector and transfected both U251 cells (to ensure continuity with the fractionation data) and mouse cortical astrocytes from nontransgenic mice. In all cell types, CTE-SUMO-1 formed into dotlike structures within the nucleus. If indeed the formation of the subnuclear dots is related to colocalization to a subnuclear structure, there were several candidates to consider. However, there are examples of sumoylated protein that are targeted to PML nuclear bodies (22, 41, 42). Furthermore, there are ~5–30 PML bodies distributed throughout the nucleus, depending on the stage of the cell cycle (43), which would give rise to a dotted appearance. Examination of primary astrocytes transfected with EGFP-CTE-SUMO-1 and counterstained with PML also revealed colocalization (Fig. 7). When transfections were carried out with an empty EGFP vector alone, the fluorescence was diffused and exclusively cytoplasmic (data not shown). To ensure that the EGFP tag was not driving the construct to the nucleus, experiments were also performed with His-CTE-SUMO-1, and similarly to the EGFP vector, the expressed construct colocalized with PML (data not shown).

PML Immunoprecipitates with CTE-SUMO in G93A Mice—Next we sought evidence of the interaction between CTE-SUMO-1 and PML through immunoprecipitation. For consistency with our previous results, we immunoprecipitated from both cytoplasmic and nuclear fractions. Since PML is almost exclusively assembled in nuclear bodies, immunocomplexes should only be detected in samples containing nuclear extracts. The ABR 518–536 antibody immunoprecipitated a band in the nuclear extract sample that was detected by the anti-PML antibody. Confirmation that this band was PML was aided by the absence of immunostaining in the cytoplasmic IP lanes (Fig. 8*A*, *top*). Fig. 8*A* (*bottom*) confirms that the His-CTE-SUMO-1 was expressed. Although the data show that PML can immunoprecipitate CTE-SUMO-1 from U251 cells, the system employs overexpression of an artificial species. Therefore, we sought to repeat the result using G93A-SOD1 end stage spinal cord lysate. Due to the limited steady amount of CTE-SUMO-1 in spinal cord nuclear extracts, we performed the immunoprecipitation from whole cell lysate. As before, the ABR 518–536 antibody immunoprecipitated a band that was detected by the anti-PML antibody. Taken together, our results suggest that the

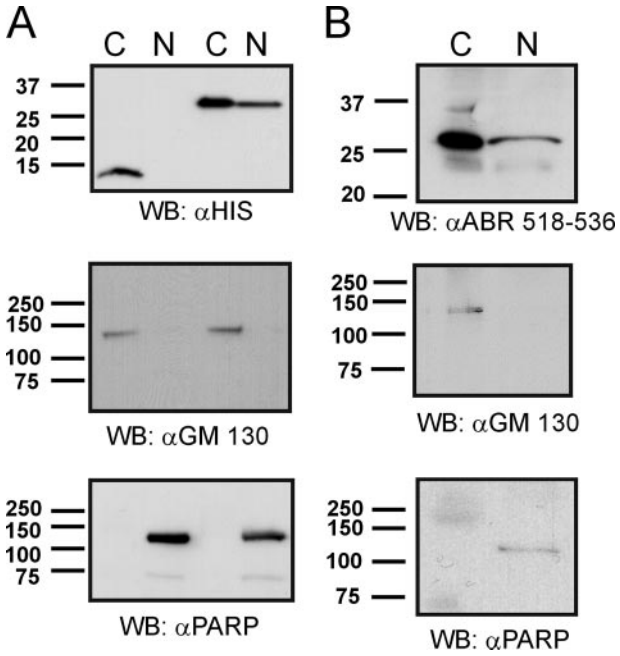

FIGURE 6. **Sumoylated CTE but not CTE can be detected in the nuclear fractions.** *A*, U251 astroglioma cells were transfected with either pcDNA3.1 His-CTE or His-CTE-SUMO-1 for 48 h before collection. Samples were separated into cytoplasmic and nuclear fractions using a Pierce NE-PER kit. 30 μg of sample was then separated on 10% gels and probed (*WB*) with antibodies against His for detection of the expressed constructs as well as for GM130 as a cytoplasmic marker and poly(ADP-ribose) polymerase (*PARP*) as a nuclear marker. *B*, G93A-SOD1 end stage mouse spinal cord homogenate was separated into cytoplasmic and nuclear fraction using a Pierce NE-PER kit. 30 μg of sample was then separated on a 10% gel and probed with ABR 518–536 antibody for detection of the EAAT2 fragment as well as for GM130 and poly(ADP-ribose) polymerase as in *A*.

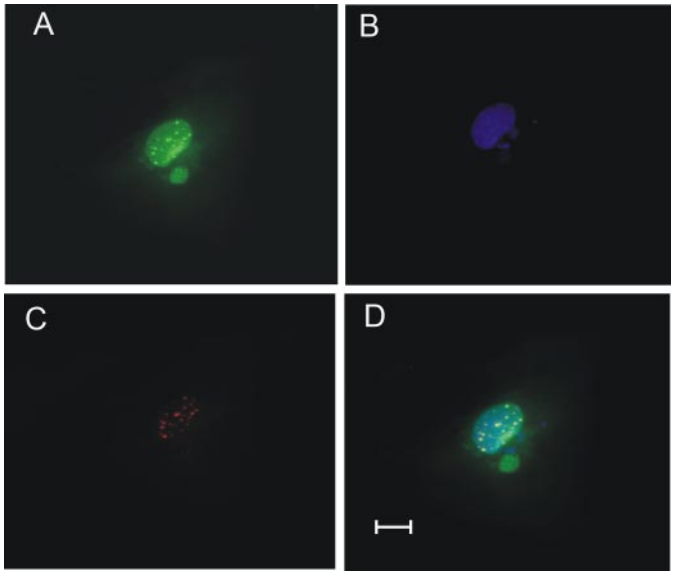

FIGURE 7. **Sumoylated CTE is localized to PML-NBs.** Spinal cord astrocytes were transfected with EGFP-CTE-SUMO-1. Immunofluorescent analysis was carried out 48 h after transfection. *A*, *green*, EGFP-CTE-SUMO-1. *B*, *blue*, DAPI. *C*, *red*, PML. PML was visualized using an anti-PML mAb from Millipore (1:200) and AlexaFluor 568 secondary anti-mouse antibody (0.5 μg/ml). *D*, merge. SUMO/DAPI/PML images were merged using Adobe Photoshop software. *Calibration bar*, 10 μm. Images indicated that CTE-SUMO-1 and PML colocalize (*yellow dots*).

sumoylated CTE species associates with PML nuclear bodies both *in vitro* and *in vivo* in the G93A-SOD1 mouse model of ALS.

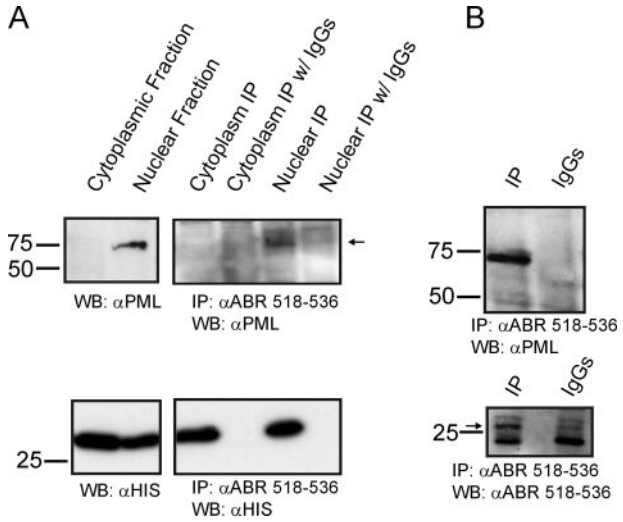

FIGURE 8. **PML is immunoprecipitated with an antibody against the COOH terminus of EAAT2.** *A*, astroglioma cells U251 were transfected with His-CTE-SUMO-1, harvested after 48 h, and separated into cytoplasmic and nuclear fractions using the NE-PER kit (Pierce). Homogenate (500 μg of protein) was immunoprecipitated (*IP*) with 10 μg of polyclonal antibody ABR 518–536. The immunoprecipitate was then separated on a 10% gel and probed (*WB*) with PML antibody (*top*). The *arrow* points at the PML band at approximately 75 kDa. The gel was also probed with anti-His antibody to ensure that transfection had taken place (*bottom*). *B*, spinal cord homogenates of diseased end stage G93A-SOD1 (500 μg of total proteins) was immunoprecipitated with 10 μg of polyclonal antibody ABR 518–536. The immunoprecipitate was then separated on a 10% gel and probed with PML antibody (*top*). As control, the immunoprecipitation was performed from a spinal cord homogenate of G93A-SOD1 end stage with 10 μg of rabbit total IgGs. The *lower panel* shows that the ABR 518–536 antibody successfully immunoprecipitated the CTE-SUMO-1 band (*arrow*) from the G93A-SOD1 spinal cord homogenates.

DISCUSSION

Decreased expression levels and impairment of the normal function of the astroglial glutamate transporter EAAT2 is a consistent feature of human ALS cases (12, 13) and animal models of the disease (44, 45). In this study, we have advanced upon our previous findings of caspase-3-mediated cleavage and inhibition of EAAT2 (16) and report that a proteolytic EAAT2 COOH terminus fragment derived from this cleavage is sumoylated. This leads to nuclear accumulation of the sumoylated EAAT2 fragment (CTE-SUMO-1) and interaction with PML in PML-NBs. During disease progression in humans and in mouse models of the disease, death of motor neurons is not accompanied by astrocyte loss. On the contrary, astrocytosis (46) and proliferation of reactive astrocytes (47) have been reported in the spinal cord of both humans and ALS mice (46, 47). Caspase-3 proteolytic cleavage of EAAT2 presumably occurs through a controlled activation of caspase-3 in astrocytes, since we observed that the cleaved EAAT2 fragment accumulates during the disease, thus negating astrocyte death. Restricted activation of caspase-3 within specific cellular compartments that is not accompanied by cell death has already been described in the literature (*e.g.* in cortical cultures exposed to ischemic preconditioning) (48). Furthermore, caspases can be activated within specific cellular compartments, as seen in neutrophils (49).

Observations obtained in both ALS mice and cell cultures also indicate that a cascade of events linked to EAAT2 process-

ing could follow the caspase-3-mediated cleavage of the transporter. In addition, Western blot analysis of homogenates of different central nervous system areas of ALS and HD mice (Fig. 5) shows that these EAAT2-linked processing mechanisms are ALS- and spinal cord-specific and fundamentally different from the EAAT2 processing occurring in HD mice, suggesting an additional level of dysregulation for this astroglial transporter. Sumoylation of a variety of different substrates under normal circumstances has important regulatory functions within the cell. We showed that the CTE fragment is conjugated to SUMO-1, an action that guards the fragment against degradation and directs it to the nucleus. One of several roles for sumoylation is to target substrate polypeptides or proteins, such as apoptin (22), BLM (41), and Sp3 (42) to PML-NBs. Once EAAT2 is cleaved, it is an inherent function of a sumoylated protein or peptide to be transported to PML-NBs. The targeting of the CTE-SUMO-1 fragment to a subnuclear structure implicated, among other processes, in transcriptional regulation might have particular significance, given a recent study in which the authors reported that astrocytes expressing G93A-SOD1 release soluble neurotoxic factors specifically detrimental to motorneurons (8). It is therefore of interest to uncover whether CTE-SUMO-1 alters astrocyte physiology, promoting release of motorneuron toxic factors.

Sumoylation of EAAT2 could be a disease-specific event. The immunoprecipitation data in Fig. 3 indicate that the homotrimer (at ~200 kDa) is sumoylated, as shown both in the forward and reverse immunoprecipitation experiments at the end stage of disease. Furthermore, Fig. 4 shows that sumoylation of the full-length transporter is possible, at least *in vitro*, in a transfected cell culture model. Functionally, the effect of sumoylation of the full-length transporter may also be relevant for the pathology. To date, there are two reports of plasma membrane ion channels that are sumoylated (24, 25). In both cases, the functional result is silencing or profound alteration of these channels. There are two other reports of sumoylation of membrane-bound proteins. Tang *et al.* (50) reported that metabotropic glutamate receptor 8a (mGluR8a) can be sumoylated, although no functional consequence of sumoylation was assigned, whereas Giorgino *et al.* (51) reported that the glucose transporters GLUT1 and GLUT4 are sumoylated in insulin-sensitive cells, resulting in differential regulation of protein levels. However, these observations were not reported in a disease context. EAAT2 does not appear to be sumoylated in wild type, nondiseased controls. Therefore, an ALS-related change in the cellular sumoylation pattern must occur, allowing EAAT2 or the proteolytic fragment derived from it to become sumoylated. Evidence in the literature suggests that the pattern of sumoylation can change with oxidative stress (52, 53), which has been described in ALS. We reported that EAAT2 is directly affected by oxidative stress in the presence of mutSOD1. Therefore, there is the possibility that in the ALS disease setting, EAAT2 could become sumoylated as a consequence of oxidative stress. If oxidative stress were to increase sumoylation, then we would expect additional proteins to become sumoylated and not just EAAT2. Thus, it is of interest to note a study by Fei *et al.* (54) reporting sumoylation of SOD1 that results in its stabilization and aggregation in familial ALS.

Given that there is clear nuclear localization and association of CTE-SUMO-1 with PML-NBs in ALS, it is likely that this fragment perturbs the dynamics of normal nuclear function in astrocytes. Current understanding indicates a role in transcription for PML-NBs, since an array of transcription factors as well as co-activators and co-repressors associate with these bodies (55). Moreover, PML-NBs are sites of action and also transcription for certain viruses (56), DNA repair (57), p53-dependent and independent apoptosis (55, 58), antiviral response (59), and cell cycle regulation (60). How PML-NBs associate with specific nuclear loci is unknown. One suggested mechanism for transcription of genes is that genomic loci are recruited to PML-NBs, and it is then that transcription is regulated. An alternate mechanism is that PML-NBs are recruited to genomic loci of high transcriptional activity, as seen with viral infections (61). An increasing number of reports are providing details of nonrandom association of PML-NBs with specific gene loci (62). What might be the result of CTE-SUMO-1 localization to PML-NBs in the context of mutSOD1-linked ALS remains to be elucidated. $PML^{-/-}$ mice are viable although more vulnerable to infection and more sensitive to carcinogens (60). Clues for the potential functional effects of CTE-SUMO-1 interaction with PML-NBs could be inferred from the analysis of these mice. However, one must consider that the result of any disruption to PML-NBs in ALS could be more complex due to the short life span of the ALS mice compared with the $PML^{-/-}$ mice and to the fact that the disruption would only occur in astrocytes.

The contribution of astrocytes to the pathology of ALS is increasingly being appreciated, particularly with the recent publication of two studies reporting non-cell autonomous effects of astrocytes carrying SOD1 mutations (7, 8). In particular, the study by Nagai *et al.* (8) suggested the existence of soluble mediators released by mutSOD1 astrocytes that are selectively toxic to motor neurons. Although the study did not indicate what these astrocyte specific mediators may be, it is of interest to note that key toxic chemokines, such as interleukin-1β, interleukin-6, interferon-γ, and tumor necrosis factor-α, were not involved. Notably, the lack of increase in tumor necrosis factor-α is in agreement with a previous study that showed that knock-out of tumor necrosis factor-α did not affect ALS caused by SOD1 mutations (63).

An attractive scenario therefore is that EAAT2 sumoylated as a result of increased cellular stress due to the presence of mutant SOD1 is progressively cleaved by caspase-3, and the sumoylated CTE species is then transported to the nucleus, where it is directed to PML-NBs. Since SUMO proteases are present within the nucleus, the novel species should not accumulate at first, but as the disease progresses and levels of the CTE-SUMO-1 increase, the balance is altered such that it allows nuclear accumulation. The role of SUMO proteases in the nucleus is probably the reason why we observe much more CTE-SUMO-1 in the cytoplasm. Obviously, the observation is more apparent when we express the fusion construct in U251 cells due to the fact that the CTE-SUMO-1 species is an in-

frame fusion and is a synthetic species with no cleavable SUMO site. The result is accumulation of sumoylated CTE at PML-NBs, where it presumably alters a facet of their normal function. In light of the observations of a non-cell autonomous effect of astrocytes on the demise of motor neurons in ALS and that the effect is seemingly due to soluble factor(s), it is tempting to speculate that our observations could reflect an underlying cause. It is our intention that the next step is to search for functional implications of CTE-SUMO-1 targeted to PML-NBs.

Acknowledgment—We are grateful to Dr. N. C. Danbolt (University of Oslo, Norway) for providing the glutamate transporter antibodies B 12–26 and B 493–508.

REFERENCES

1. Gurney, M. E., Pu, H., Chiu, A. Y., Dal Canto, M. C., Polchow, C. Y., Alexander, D. D., Caliendo, J., Hentati, A., Kwon, Y. W., Deng, H. X., Chen, W., Zhai, P., Sufit, R. L., and Siddique, T. (1994) *Science* **264,** 1772–1775
2. Howland, D. S., Liu, J., She, Y., Goad, B., Maragakis, N. J., Kim, B., Erickson, J., Kulik, J., DeVito, L., Psaltis, G., DeGennaro, L. J., Cleveland, D. W., and Rothstein, J. D. (2002) *Proc. Natl. Acad. Sci. U. S. A.* **99,** 1604–1609
3. Taylor, A. R., Gifondorwa, D. J., Newbern, J. M., Robinson, M. B., Strupe, J. L., Prevette, D., Oppenheim, R. W., and Milligan, C. E. (2007) *J. Neurosci.* **27,** 634–644
4. Danbolt, N. C. (2001) *Prog. Neurobiol.* **65,** 1–105
5. Boillee, S., Yamanaka, K., Lobsiger, C. S., Copeland, N. G., Jenkins, N. A., Kassiotis, G., Kollias, G., and Cleveland, D. W. (2006) *Science* **312,** 1389–1392
6. Clement, A. M., Nguyen, M. D., Roberts, E. A., Garcia, M. L., Boillee, S., Rule, M., McMahon, A. P., Doucette, W., Siwek, D., Ferrante, R. J., Brown, R. H., Jr., Julien, J.-P., Goldstein, L. S. B., and Cleveland, D. W. (2003) *Science* **302,** 113–117
7. Di Giorgio, F. P., Carrasco, M. A., Siao, M. C., Maniatis, T., and Eggan, K. (2007) *Nat. Neurosci.* **10,** 608–614
8. Nagai, M., Re, D. B., Nagata, T., Chalazonitis, A., Jessell, T. M., Wichterle, H., and Przedborski, S. (2007) *Nat. Neurosci.* **10,** 615–622
9. Pehar, M., Cassina, P., Vargas, M. R., Castellanos, R., Viera, L., Beckman, J. S., Estevez, A. G., and Barbeito, L. (2004) *J. Neurochem.* **89,** 464–473
10. Boillee, S., Vande Velde, C., and Cleveland, D. W. (2006) *Neuron* **52,** 39–59
11. Pasinelli, P., and Brown, R. H. (2006) *Nat. Rev. Neurosci.* **7,** 710–723
12. Lin, C.-L. G., Bristol, L. A., Jin, L., Dykes-Hoberg, M., Crawford, T., Clawson, L., and Rothstein, J. D. (1998) *Neuron* **20,** 589–602
13. Rothstein, J. D., Van Kammen, M., Levey, A. I., Martin, L. J., and Kuncl, R. W. (1995) *Ann. Neurol.* **38,** 73–84
14. Guo, H., Lai, L., Butchbach, M. E., Stockinger, M. P., Shan, X., Bishop, G. A., and Lin, C. L. (2003) *Hum. Mol. Genet.* **12,** 2519–2532
15. Pardo, A. C., Wong, V., Benson, L. M., Dykes, M., Tanaka, K., Rothstein, J. D., and Maragakis, N. J. (2006) *Exp. Neurol.* **201,** 120–130
16. Boston-Howes, W., Gibb, S. L., Williams, E. O., Pasinelli, P., Brown, R. H., Jr., and Trotti, D. (2006) *J. Biol. Chem.* **281,** 14076–14084
17. Hay, R. T. (2005) *Mol. Cell* **18,** 1–12
18. Sampson, D. A., Wang, M., and Matunis, M. J. (2001) *J. Biol. Chem.* **276,** 21664–21669
19. Chung, T. L., Hsiao, H. H., Yeh, Y. Y., Shia, H. L., Chen, Y. L., Liang, P. H., Wang, A. H., Khoo, K. H., and Shoei-Lung Li, S. (2004) *J. Biol. Chem.* **279,** 39653–39662
20. Melchior, F., Schergaut, M., and Pichler, A. (2003) *Trends Biochem. Sci.* **28,** 612–618
21. Desterro, J. M., Rodriguez, M. S., and Hay, R. T. (1998) *Mol. Cell* **2,** 233–239
22. Janssen, K., Hofmann, T. G., Jans, D. A., Hay, R. T., Schulze-Osthoff, K., and Fischer, U. (2007) *Oncogene* **26,** 1557–1566
23. Muller, S., Berger, M., Lehembre, F., Seeler, J. S., Haupt, Y., and Dejean, A. (2000) *J. Biol. Chem.* **275,** 13321–13329
24. Rajan, S., Plant, L. D., Rabin, M. L., Butler, M. H., and Goldstein, S. A. (2005) *Cell* **121,** 37–47
25. Benson, M. D., Li, Q. J., Kieckhafer, K., Dudek, D., Whorton, M. R., Sunahara, R. K., Iniguez-Lluhi, J. A., and Martens, J. R. (2007) *Proc. Natl. Acad. Sci. U. S. A.* **104,** 1805–1810
26. Joseph, J., Tan, S. H., Karpova, T. S., McNally, J. G., and Dasso, M. (2002) *J. Cell Biol.* **156,** 595–602
27. Shen, T. H., Lin, H. K., Scaglioni, P. P., Yung, T. M., and Pandolfi, P. P. (2006) *Mol. Cell* **24,** 331–339
28. Dorval, V., and Fraser, P. E. (2007) *Biochim. Biophys. Acta* **1773,** 694–706
29. Nagai, M., Aoki, M., Miyoshi, I., Kato, M., Pasinelli, P., Kasai, N., Brown, R. H., Jr., and Itoyama, Y. (2001) *J. Neurosci.* **21,** 9246–9254
30. Holmseth, S., Dehnes, Y., Bjornsen, L. P., Boulland, J. L., Furness, D. N., Bergles, D., and Danbolt, N. C. (2005) *Neuroscience* **136,** 649–660
31. Holmseth, S., Lehre, K. P., and Danbolt, N. C. (2006) *Anat. Embryol.* (*Berl.*) **211,** 257–266
32. Danbolt, N. C., Lehre, K. P., Dehnes, Y., Chaudhry, F. A., and Levy, L. M. (1998) *Methods Enzymol.* **296,** 388–407
33. Gyuris, J., Golemis, E., Chertkov, H., and Brent, R. (1993) *Cell* **75,** 791–803
34. Yernool, D., Boudker, O., Jin, Y., and Gouaux, E. (2004) *Nature* **431,** 811–818
35. Neumar, R. W., Xu, Y. A., Gada, H., Guttmann, R. P., and Siman, R. (2003) *J. Biol. Chem.* **278,** 14162–14167
36. Antoine, K., Prosperi, M. T., Ferbus, D., Boule, C., and Goubin, G. (2005) *Mol. Cell. Biochem.* **271,** 215–223
37. Steffan, J. S., Agrawal, N., Pallos, J., Rockabrand, E., Trotman, L. C., Slepko, N., Illes, K., Lukacsovich, T., Zhu, Y. Z., Cattaneo, E., Pandolfi, P. P., Thompson, L. M., and Marsh, J. L. (2004) *Science* **304,** 100–104
38. Iwabuchi, K., Li, B., Bartel, P., and Fields, S. (1993) *Oncogene* **8,** 1693–1696
39. Li, B., and Fields, S. (1993) *FASEB J.* **7,** 957–963
40. Lievens, J. C., Woodman, B., Mahal, A., Spasic-Boscovic, O., Samuel, D., Kerkerian-Le Goff, L., and Bates, G. P. (2001) *Neurobiol. Dis.* **8,** 807–821
41. Eladad, S., Ye, T. Z., Hu, P., Leversha, M., Beresten, S., Matunis, M. J., and Ellis, N. A. (2005) *Hum. Mol. Genet.* **14,** 1351–1365
42. Ross, S., Best, J. L., Zon, L. I., and Gill, G. (2002) *Mol. Cell* **10,** 831–842
43. Zhong, S., Salomoni, P., and Pandolfi, P. P. (2000) *Nat. Cell Biol.* **2,** E85–E90
44. Bruijn, L. I., Becher, M. W., Lee, M. K., Anderson, K. L., Jenkins, N. A., Copeland, N. G., Sisodia, S. S., Rothstein, J. D., Borchelt, D. R., Price, D. L., and Cleveland, D. W. (1997) *Neuron* **18,** 327–338
45. Bendotti, C., Tortarolo, M., Suchak, S. K., Calvaresi, N., Carvelli, L., Bastone, A., Rizzi, M., Rattray, M., and Mennini, T. (2001) *J. Neurochem.* **79,** 737–746
46. Johansson, A., Engler, H., Blomquist, G., Scott, B., Wall, A., Aquilonius, S. M., Langstrom, B., and Askmark, H. (2007) *J. Neurol. Sci.* **255,** 17–22
47. Schiffer, D., Cordera, S., Cavalla, P., and Migheli, A. (1996) *J. Neurol. Sci.* **139,** (suppl.) 27–33
48. McLaughlin, B., Hartnett, K. A., Erhardt, J. A., Legos, J. J., White, R. F., Barone, F. C., and Aizenman, E. (2003) *Proc. Natl. Acad. Sci. U. S. A.* **100,** 715–720
49. Pederzoli, M., Kantari, C., Gausson, V., Moriceau, S., and Witko-Sarsat, V. (2005) *J. Immunol.* **174,** 6381–6390
50. Tang, Z., El Far, O., Betz, H., and Scheschonka, A. (2005) *J. Biol. Chem.* **280,** 38153–38159
51. Giorgino, F., de Robertis, O., Laviola, L., Montrone, C., Perrini, S., McCowen, K. C., and Smith, R. J. (2000) *Proc. Natl. Acad. Sci. U. S. A.* **97,** 1125–1130
52. Manza, L. L., Codreanu, S. G., Stamer, S. L., Smith, D. L., Wells, K. S., Roberts, R. L., and Liebler, D. C. (2004) *Chem. Res. Toxicol.* **17,** 1706–1715
53. Zhou, W., Ryan, J. J., and Zhou, H. (2004) *J. Biol. Chem.* **279,** 32262–32268
54. Fei, E., Jia, N., Yan, M., Ying, Z., Sun, Q., Wang, H., Zhang, T., Ma, X., Ding, H., Yao, X., Shi, Y., and Wang, G. (2006) *Biochem. Biophys. Res. Commun.* **347,** 406–412

55. Guo, A., Salomoni, P., Luo, J., Shih, A., Zhong, S., Gu, W., and Pandolfi, P. P. (2000) *Nat. Cell Biol.* **2,** 730–736
56. Everett, R. D. (2001) *Oncogene* **20,** 7266–7273
57. Dellaire, G., and Bazett-Jones, D. P. (2004) *BioEssays* **26,** 963–977
58. Wang, Z. G., Ruggero, D., Ronchetti, S., Zhong, S., Gaboli, M., Rivi, R., and Pandolfi, P. P. (1998) *Nat. Genet.* **20,** 266–272
59. Regad, T., and Chelbi-Alix, M. K. (2001) *Oncogene* **20,** 7274–7286
60. Wang, Z. G., Delva, L., Gaboli, M., Rivi, R., Giorgio, M., Cordon-Cardo, C., Grosveld, F., and Pandolfi, P. P. (1998) *Science* **279,** 1547–1551
61. Ching, R. W., Dellaire, G., Eskiw, C. H., and Bazett-Jones, D. P. (2005) *J. Cell Sci.* **118,** 847–854
62. Sun, Y., Durrin, L. K., and Krontiris, T. G. (2003) *Genomics* **82,** 250–252
63. Gowing, G., Dequen, F., Soucy, G., and Julien, J. P. (2006) *J. Neurosci.* **26,** 11397–11402

A Caspase-3-cleaved Fragment of the Glial Glutamate Transporter EAAT2 Is Sumoylated and Targeted to Promyelocytic Leukemia Nuclear Bodies in Mutant SOD1-linked Amyotrophic Lateral Sclerosis

Stuart L. Gibb, William Boston-Howes, Zeno S. Lavina, Stefano Gustincich, Robert H. Brown, Jr., Piera Pasinelli and Davide Trotti

J. Biol. Chem. 2007, 282:32480-32490.
doi: 10.1074/jbc.M704314200 originally published online September 6, 2007
